

Bat-borne H9N2 influenza virus evades MxA restriction and exhibits efficient replication and transmission in ferrets

Received: 20 December 2023

Accepted: 27 March 2024

Published online: 25 April 2024

Check for updates

Nico Joel Halwe¹, Lea Hamberger^{2,3}, Julia Sehl-Ewert⁴, Christin Mache⁵, Jacob Schön¹, Lorenz Ulrich¹, Sten Calvelage¹, Mario Tönnies⁶, Jonas Fuchs^{2,3}, Pooja Bandawane^{7,8}, Madhumathi Loganathan^{7,8}, Anass Abbad^{7,8}, Juan Manuel Carreño^{7,8}, Maria C. Bermúdez-González^{7,8}, Viviana Simon^{7,8,9,10,11}, Ahmed Kandeil^{12,13}, Rabeh El-Shesheny^{12,13}, Mohamed A. Ali¹², Ghazi Kayali^{12,13}, Matthias Budt⁵, Stefan Hippenstiel¹⁴, Andreas C. Hocke¹⁴, Florian Krammer^{7,8,9}, Thorsten Wolff⁵, Martin Schwemmler^{2,3}, Kevin Ciminski^{2,3}✉, Donata Hoffmann¹✉ & Martin Beer¹✉

Influenza A viruses (IAVs) of subtype H9N2 have reached an endemic stage in poultry farms in the Middle East and Asia. As a result, human infections with avian H9N2 viruses have been increasingly reported. In 2017, an H9N2 virus was isolated for the first time from Egyptian fruit bats (*Rousettus aegyptiacus*). Phylogenetic analyses revealed that bat H9N2 is descended from a common ancestor dating back centuries ago. However, the H9 and N2 sequences appear to be genetically similar to current avian IAVs, suggesting recent reassortment events. These observations raise the question of the zoonotic potential of the mammal-adapted bat H9N2. Here, we investigate the infection and transmission potential of bat H9N2 in vitro and in vivo, the ability to overcome the antiviral activity of the human MxA protein, and the presence of N2-specific cross-reactive antibodies in human sera. We show that bat H9N2 has high replication and transmission potential in ferrets, efficiently infects human lung explant cultures, and is able to evade antiviral inhibition by MxA in transgenic B6 mice. Together with its low antigenic similarity to the N2 of seasonal human strains, bat H9N2 fulfils key criteria for pre-pandemic IAVs.

Influenza A viruses (IAVs) are highly infectious viral pathogens that can cross interspecies barriers and infect a wide range of avian and mammalian species¹. Although bats have long been known to be reservoirs for a variety of viruses², they were only recently found to also harbor IAVs^{3,4}. While H17N10 and H18N11 strains were first identified in Central and South American bat species^{3,4}, the H9N2 virus A/bat/Egypt/3810P/2017, designated as bat H9N2, was recently isolated from Egyptian fruit bats (*Rousettus aegyptiacus*) in the Nile Delta region⁵. Phylogenetic analyses suggest that this Old World bat H9N2 virus is distinct from the

New World bat IAVs H17N10 and H18N11, and emerged as a reassortant from an ancestral bat backbone and avian IAV H9 and N2 segments⁶. Avian H9N2 viruses were first isolated from turkeys in North American poultry farms in 1966⁷ and subsequently became endemic in poultry farms in many countries in the Middle East and Asia^{8,9}. Since then, avian H9N2 viruses have become widespread and have undergone extensive reassortment with other circulating avian IAVs, resulting in at least 74 different lineages¹⁰. Over the past two decades, avian H9N2 infections have been recorded in swine populations and mink farms^{11,12}.

A full list of affiliations appears at the end of the paper. ✉ e-mail: kevin.ciminski@uniklinik-freiburg.de; donata.hoffmann@fli.de; martin.beer@fli.de

Furthermore, since 1998, the WHO has reported 82 human spill-over infections with avian IAVs in China or Cambodia, resulting in mild to severe disease¹³. Interestingly, sero-epidemiological data from Ghanaian straw-colored fruit bats showed a high prevalence of H9-specific antibodies (30%)¹⁴, and bat H9N2 was also detected in Egyptian fruit bats from South Africa¹⁵, suggesting widespread circulation of bat H9N2 in African bat populations. Similar to avian H9N2, bat H9N2 initiates infection by utilizing avian IAV-like $\alpha 2,3$ sialic acid receptors, and replicates in mice, but not in adult chickens⁵. Here, we investigated whether bat H9N2 is of zoonotic concern. We show that the bat H9N2 IAV isolated from Egyptian fruit bats exhibits robust replication and transmission in ferrets, effectively infects human lung cells, evades MxA antiviral activity, and has low antigenic similarity to seasonal human strains, indicating its potential as a pre-pandemic influenza strain.

Results and discussion

As H9N2 viruses were originally isolated from turkeys⁷, we first determined the replication properties of bat H9N2 in 1-day-old turkeys. Following oro-nasal inoculation, bat H9N2 replicated efficiently to 10^5 – 10^7 copies mL^{-1} at 1 day post infection (dpi; Supplementary Fig. 1a). Thereafter, viral loads rapidly decreased but again reached titers of 5×10^5 copies mL^{-1} between 5 and 8 dpi. Infectious virus was isolated from oral swabs collected at 5 dpi (Supplementary Fig. 1a). At 11 dpi, all but one oral swab was negative for viral RNA (Supplementary Fig. 1a) and no viral RNA was detected in cloacal swabs at any time point measured. All turkey hatchlings seroconverted with antibodies targeting the viral nucleoprotein (NP) at 21 dpi (Supplementary Fig. 1b, c), demonstrating that bat H9N2 maintained its ability to replicate in turkeys. In contrast, and in agreement with previous reports⁵, bat H9N2 failed to replicate efficiently in 1-day-old chicken and did not elicit an antibody response (Supplementary Fig. 1d, e). In the future, the molecular species differences that allow the bat H9N2 to replicate efficiently in turkeys but not chickens need to be investigated in more detail.

In order to assess the zoonotic potential and transmissibility of bat H9N2 in the model most relevant to humans, we infected 15 donor ferrets and co-housed three naïve contact animals from 1 to 12 dpi (Fig. 1a and Supplementary Fig. 1f). Quantification of viral RNA obtained from nasal lavages revealed substantial viral replication (10^6 – 10^8 copies mL^{-1}) within the first 2 days after infection and continuous shedding of viral genomes and infectious virus up to 8 dpi (Fig. 1a and Supplementary Fig. 1g). Strikingly, all contact animals acquired a viral infection from donor ferrets after co-housing with peak titers (10^7 copies mL^{-1}) at 4 days post exposure (dpe) (Fig. 1a). To determine whether bat H9N2 replication is limited to the upper respiratory tract, we next measured viral titers in the organs of six donor ferrets euthanized at 6 dpi (Fig. 1b). While all ferrets had substantial viral genome copies in the nasal conchae and five of six animals had moderate levels in the trachea, one of six ferrets had moderate viral genome levels in the cranial lung lobe, two in the medial and caudal lung lobes, and one ferret even had low viral copies in the colon (Fig. 1b). We did not observe severe body weight loss in most donor and any contact ferrets, although two donor animals exhibited ~15% weight loss at 6 and 12 dpi (Fig. 1c), which was most likely unrelated to infection. Elevated body temperatures were observed at 2 dpi in 14 of 15 donor ferrets (Fig. 1d) and all contact animals had elevated body temperatures at 1 dpe (Fig. 1d). Seroconversion with NP-specific antibodies was detected as early as 6 dpi in donor ferrets, and all donor and contact ferrets examined at 21 dpi exhibited a robust NP-specific antibody response (Fig. 1e). Furthermore, at 21 dpi we determined antibodies with a strong neutralizing capacity against bat H9N2 and some degree of cross-neutralization against the avian H9N2 A/layer chicken/Bangladesh/VP02-plaque/2016 isolate (Fig. 1f). Histopathological examination revealed severe purulent to necrotizing rhinitis with

viral antigen in the epithelia of the respiratory and olfactory tract in all infected ferrets at 6 dpi (Fig. 1g). We observed mild infection-induced changes characterized by focal to oligofocal epithelial necrosis and mild infiltration of the lamina propria in the trachea of four animals. In accordance with the low viral genome copies detected in the ferret lungs, no influenza-associated lung pathology was detected, which is in contrast to lung pathology of ferrets after infection with e.g. reassorted H9N2- or highly pathogenic avian influenza strains^{16–19}.

Because severe courses of influenza in humans almost always affect the lower respiratory tract²⁰, we next infected human ex vivo lung cultures with bat H9N2, a prototypic human seasonal H3N2 isolate (A/Panama/2007/1999) or chicken H9N2 and determined viral growth properties. Intriguingly, bat H9N2 replicated to comparable or even higher viral titers than human H3N2, reaching peak titers of 3×10^4 plaque-forming units (PFU) mL^{-1} at 48 h post infection (hpi; Fig. 2a). In contrast, chicken H9N2 showed minimal viral replication in human lung tissue. Immunostaining of lung explants at 24 hpi revealed that all viruses infected alveolar type II cells (Fig. 2b), which is the primary cellular tropism of IAV in the lung²¹.

Next, we studied whether bat H9N2 is able to escape human MxA, a crucial innate antiviral factor which restricts IAVs by inhibiting their polymerase activity²². Human-adapted IAVs, such as the pandemic H1N1 virus A/Hamburg/4/2009 (pdmH1N1), acquire characteristic clusters of adaptive mutations in NP that enable escape from MxA^{22,23}, whereas such clusters are virtually absent in IAVs of avian origin including the highly pathogenic H5N1 strain A/Thailand/1(KAN-1)/2004 (KAN-1). Bat H9N2 NP also lacks the residues described as conferring MxA resistance (Supplementary Fig. 2a). Thus, as expected, bat H9N2 exhibited a high degree of MxA-sensitivity as demonstrated by infecting MDCK cells stably overexpressing either wild-type MxA (MDCK-MxA) or the antivirally inactive MxA_{T103A} variant (MDCK-MxA_{T103A})²⁴. While pdmH1N1, KAN-1 and bat H9N2 replicated efficiently in MDCK-MxA_{T103A} cells to titers between 1.3×10^7 and 7×10^8 PFU mL^{-1} at 48 hpi (Fig. 2c), KAN-1 was nearly completely inhibited in MDCK-MxA cells whereas peak titers of pdmH1N1 decreased only 5-fold. Replication of bat H9N2 was potently restricted in the presence of MxA as illustrated by residual viral titers $\leq 10^2$ PFU mL^{-1} between 24–48 hpi (Fig. 2c).

To assess the importance of MxA in controlling bat H9N2 in vivo, we intranasally infected wild type C57BL/6 (B6), which lack a functional Mx protein, and human MxA-transgenic (hMxA^{tg/tg}) mice with bat H9N2. Surprisingly, lung viral titers were similar in both B6 and MxA-transgenic mice²⁵ at 3 dpi (5×10^5 PFU mL^{-1} ; Fig. 2d), as confirmed by comparable NP levels in lung homogenates detected by Western blotting (Fig. 2f). Interestingly, MxA expression was not observed in the lungs of infected hMxA^{tg/tg} mice, but could be potently induced by IFN- α pretreatment 18 h prior to challenge infection with bat H9N2. Under these conditions, we observed induction of MxA (Fig. 2f) and 10-fold lower lung viral lung titers in hMxA^{tg/tg} compared to B6 mice (Fig. 2e), suggesting that MxA, when induced, reduces bat H9N2 replication.

Finally, because there is little serological evidence for H9-specific antibodies in the human population^{26,27}, we wondered whether the antibody responses to circulating seasonal H1N1 and H3N2 strains as well as vaccination would be cross-reactive for bat N2. Serum collected from 15 healthy adults before and after seasonal influenza vaccination in 2022/23 revealed no reactivity to bat N2 (Supplementary Fig. 2b,e), but robust reactivity to N2 from the seasonal A/Kansas/14/2017 (H3N2) isolate (Supplementary Fig. 2d).

Our study shows that the Old World bat H9N2 virus meets key characteristics of a pre-pandemic IAV, including replication in and efficient transmission between ferrets, the ability to replicate efficiently in human lung explants and evasion from MxA-mediated restriction. Intriguingly, bat H9N2 exhibits an immediate (at 1 dpe) and highly efficient transmission potential (100%) not previously observed

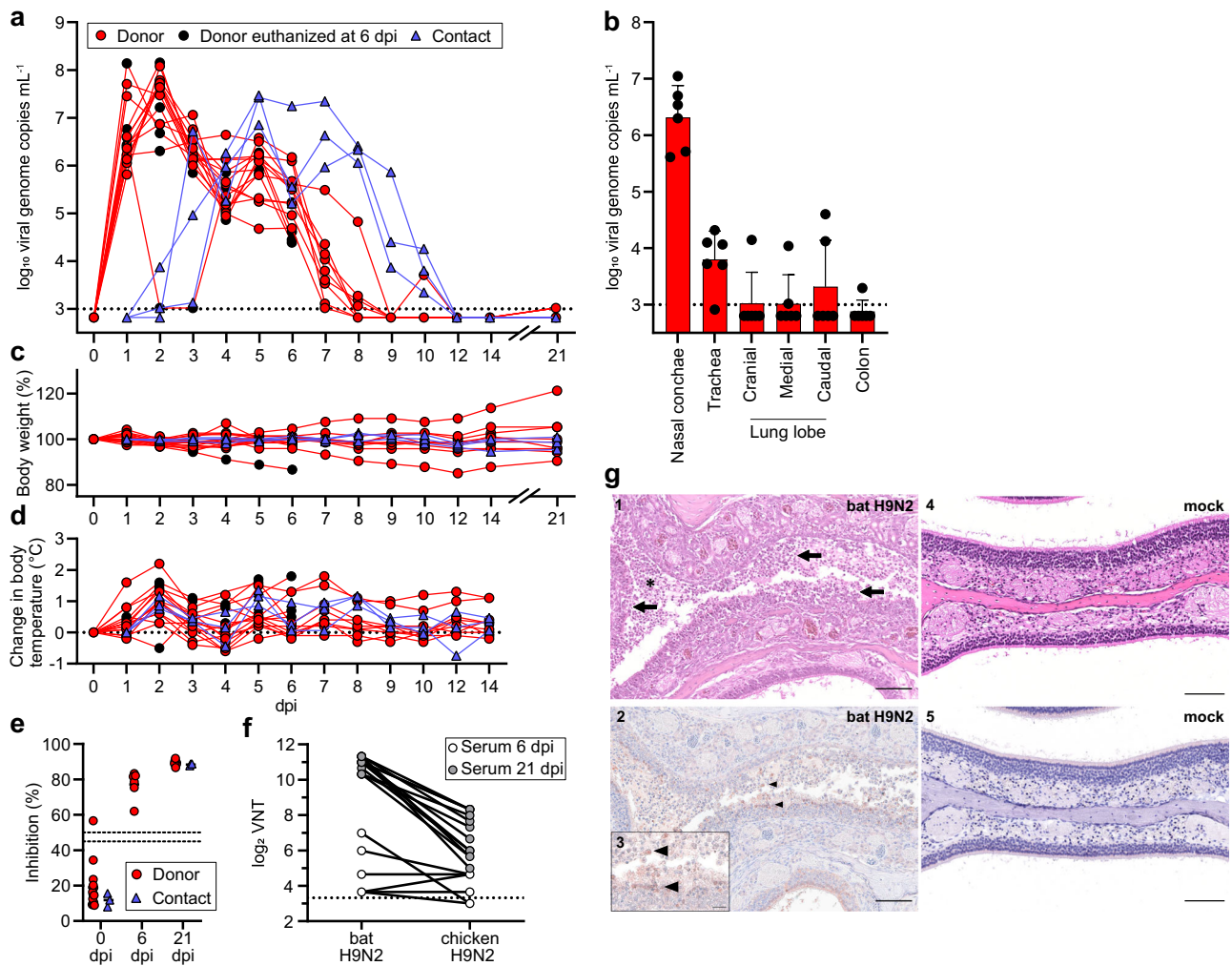


Fig. 1 | Ferrets are highly susceptible to bat H9N2. **a** Ferrets ($n = 15$) were inoculated with $10^{4.8}$ TCID₅₀ of bat H9N2 IAV per animal. At 1 dpi, direct contact animals ($n = 3$) were co-housed. Donor ferrets euthanized at 6 dpi are indicated. Viral shedding was measured by nasal lavage. Dashed line indicates detection limit. **b** Organs collected from euthanized ferrets ($n = 6$) at 6 dpi with bat H9N2 were tested by RT-qPCR to determine viral genome copies. Dashed line indicates detection limit. Data are mean \pm SD. **c** Changes in body weight relative to 0 dpi of bat H9N2-infected ($n = 15$) and contact ($n = 3$) ferrets were monitored throughout the course of the experiment. **d** Changes from the baseline body temperatures of donor and naïve contact ferrets were monitored from 0 to 14 dpi. **e** Ferret serum antibody titers in an IAV NP-specific ELISA at the indicated time points (0 dpi $n = 18$, 6 dpi $n = 6$, 21 dpi $n = 12$). Dashed lines indicate threshold between 45% and 50% inhibition. Mean antibody titers are indicated. Note that one ferret showed weak

reactivity in the pre-experimental NP-ELISA, but was included in the study because of its low seropositivity, which could be due to a previously unrecognized IAV infection or an unspecific ELISA reactivity. There was no indication of H9N2 serology prior to inoculation. **f** Ferret neutralizing antibody titers ($n = 18$) against bat H9N2 and chicken H9N2. **g** Histopathologic findings with detection of viral antigen in the nasal mucosa of bat H9N2-infected ferrets ($n = 6$, panels 1–3) at 6 dpi or mock-infected ferret ($n = 1$, panels 4 and 5). Acute severe rhinitis with diffuse necrosis of the olfactory epithelium (arrow) and infiltrating neutrophils (asterisk) (1). Intralosomal viral antigen (NP) is abundant in degenerated and desquamated epithelial cells (arrowhead) (2). The inset (3) is a higher magnification of the center of the image (2). No pathology was observed in the mock-infected ferret (4, 5). Representative images are shown. Scale bar, 100 μ m (main panels), 25 μ m (inset). Source data are provided as a Source Data file.

in any avian-derived H9N2 isolate with an α 2,3 sialic acid receptor specificity^{28–31}. As the bat H9N2 HA specifically binds to avian IAV-like α 2,3 sialic acid receptors for cell entry and fails to recognize mammalian-like α 2,6 sialic acid receptors⁵, we suggest that infection of ferrets and mice occurs by binding to α 2,3 sialic acid receptors, which are also present in low numbers in the upper respiratory tract^{32,33}. Thus, the ability of bat H9N2 to replicate in and transmit among ferrets may also allow for spread among and further adaptation to humans. Our data also suggests that bat H9N2 can suppress the expression of MxA, thereby overcoming this important restriction factor for zoonotic spill-over³⁴. This is in strong contrast to zoonotic H5N1 and H7N9 viruses of avian origin, which also lack MxA resistance in NP but induce MxA in hMxA^{tg/tg} mice and thus are potentially inhibited²⁵. Given the ability of bat H9N2 to infect turkey hatchlings, introduction of bat H9N2 into poultry farms and reassortment with avian IAV cannot be ruled out,

necessitating increased attention and close monitoring of possible human spill-over infections in Africa.

A further prerequisite of pre-pandemic viruses is their antigenic novelty to the human immune system. Since the human population is presently exposed only to the currently-circulating H1N1 and H3N2 subtypes, a lack of humoral immunity to bat H9N2 is very likely. Indeed, our serological data demonstrates that seasonal influenza vaccines containing H1N1 and H3N2 do not elicit cross-reactive antibodies to the bat N2 protein, substantiating the general pre-pandemic features of bat H9N2.

Methods

Virus

The bat-derived H9N2 A/bat/Egypt/381OP/2017 isolate (GenBank accession numbers: MH376902 to MH376909), was propagated in

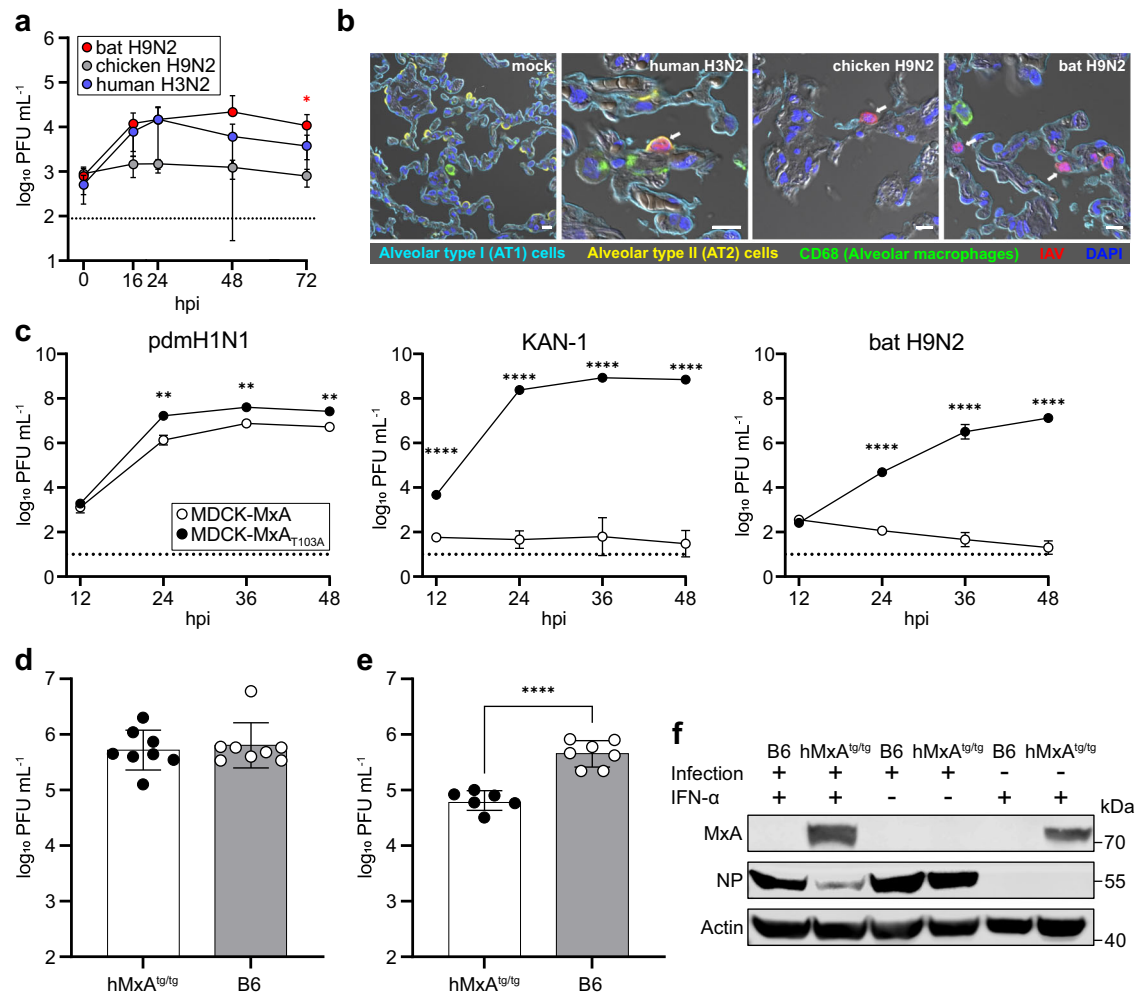


Fig. 2 | Bat H9N2 replicates in human lung explants and suppresses induction of MxA in MxA-transgenic mice. **a** Human lung tissue explants ($n = 4$) were infected with human H3N2, chicken H9N2 or bat H9N2 with 1×10^6 PFU, and viral titers were determined at the indicated time points. Error bars indicate standard deviation and statistical analysis was performed using non-paired, non-parametric Kruskal-Wallis test ($^*p = 0.0324$). Data are mean \pm SD of $n = 4$ independent experiments. Dashed line indicates detection limit **(b)** At 24 hpi, human lung explants were stained for alveolar type I (AT1) (cyan) and type II (AT2) cells (yellow), CD68 indicating alveolar macrophages (green) and IAV antigens (red). Note, in chicken H9N2 and bat H9N2 infected cells, AT2 labeling was omitted for better visualization. White arrows indicate infected cells. Scale bar, 10 μ m. **c** MDCK cells over-expressing MxA or inactive MxA_{T103A} were infected with human-adapted pdmH1N1,

avian KAN-1 (H5N1) or bat H9N2 at an MOI of 0.001, and viral titers were determined at the indicated time points. Data are mean \pm SD of $n = 3$ independent experiments; statistical analysis was performed using two-tailed *t*-tests; $^{**}P = 0.01$; $^{****}P = 0.0001$. Dashed line indicates detection limit. **d** hMxA^{tg/tg} ($n = 8$) or wild-type B6 mice ($n = 8$) were infected with 1×10^4 PFU. Lung viral titers were determined 3 dpi. **e** hMxA^{tg/tg} ($n = 6$) or wild-type B6 mice ($n = 7$) were pretreated with IFN- α 18 h prior to infection with 1×10^4 PFU. Lung viral titers were determined 3 dpi. Data are mean \pm SD; statistical analysis was performed using two-tailed *t*-tests; $^{****}P = 0.0001$. **f** MxA, NP and actin protein levels in homogenized lungs from IFN- α pretreated or infected mice from **(d,e)** were detected by Western blot. Source data are provided as a Source Data file.

embryonated SPF-chicken eggs for 5 days at 37 °C. Subsequently, the allantoic fluid was harvested and used as virus stock. The chicken H9N2 isolate A/layer chicken/Bangladesh/VP02-plaque/2016 was obtained from the Friedrich-Loeffler-Institut (FLI) virus repository³⁵. Virus stocks of the human seasonal A/Panama/2007/1999 (H3N2) isolate were generated by propagation on MDCKII cells. Recombinant A/Hamburg/4/2009 (pdmH1N1) and A/Thailand/1(KAN-1)/2004 (H5N1) were generated utilizing the eight-plasmid pHW2000-based rescue system³⁶. All recombinant viruses were plaque purified and then used for stock generation. Stock titers were determined by a plaque assay on MDCKII cells.

Cells

Madin-Darby Canine Kidney (MDCK) type II cells (Collection of Cell Lines in Veterinary Medicine CCLV RIE1061) were used. Cells were incubated at 37 °C under 5% CO₂ atmosphere using a mixture of equal

volumes of Eagle Minimum Essential Medium (MEM) (Hank's balanced salts solution) and Eagle MEM (Earle's balanced salts solution), 2 mM L-Gln, nonessential amino acids, adjusted to 850 mg L⁻¹ NaHCO₃, 120 mg L⁻¹ sodium pyruvate, pH 7.2 with 10% FCS (Bio & Sell GmbH) or without FCS in the presence of tosylsulfonyl phenylalanyl chloromethyl ketone (TPCK)-treated trypsin (Sigma) after virus addition. MDCK-MxA and MDCK-MxA_{T103A} cells were obtained by Jesse D. Bloom (Fred Hutchinson Cancer Research Center, United States)²⁴ and were cultured in Dulbecco's modified Eagle's medium (DMEM, Gibco, Thermo Fisher Scientific) containing 10% fetal calf serum (FCS), 100 U penicillin and 100 μ g streptomycin mL⁻¹ at 37 °C and 5% CO₂.

Virus infections

MDCK-MxA and MDCK-MxA_{T103A} cells were seeded and grown in 6-well plates. Prior to infection cells were washed with phosphate buffered saline (PBS) containing 0.2% bovine serum albumin (BSA) and

then infected with the indicated virus at an MOI of 0.001 in infection medium (DMEM, containing 0.2% BSA and 100 U penicillin and 100 μg streptomycin μL^{-1}). For bat H9N2 and pdmH1N1 1 μg mL^{-1} TPCK-treated trypsin was added into the infection medium. Viral titers were determined by plaque assay.

Infection of human lung explants

Fresh lung explants were obtained from patients suffering from lung carcinoma and undergoing lung resection at local thoracic surgeries. Written informed consent was obtained from all patients and the study was approved by the ethics committee at the Charité clinic (project EA2/079/13). Tumor-free peripheral lung tissue was cut into small pieces and incubated overnight at 37 °C with 5% CO_2 in Roswell Park Memorial Institute (RPMI) 1640 medium. The next day, lung tissue was infected with 1×10^6 PFU of either human seasonal H3N2, chicken H9N2 or bat H9N2 for 1.5 h under shaking conditions and excess virus was removed by three washing steps with PBS. Infected lung tissues were incubated at 37 °C and 5% CO_2 for up to 72 h in RPMI 1640 medium supplemented with 2 mM L-glutamine and 0.3% BA. Viral titers were determined by plaque assay.

Western blot

Mouse lung samples were incubated at 95 °C in Laemmli buffer and subsequently separated by sodium dodecyl sulfate polyacrylamide gel electrophoresis (SDS-PAGE). Separated protein samples were blotted onto a nitrocellulose membrane. Proteins were detected using specific antibodies against the highly conserved G domain in MxA (MI43)23, NP (Gene Tex, GTX125989, 1:1,000), or actin (Sigma-Aldrich, A3853; 1:1,000), respectively. Primary antibodies were detected using peroxidase-conjugated secondary antibodies (Jackson ImmunoResearch, 1:5,000).

Animal experiment ethics declarations

All ferret and hatchling experiments were evaluated by the responsible ethics committee of the State Office of Agriculture, Food Safety, and Fishery in Mecklenburg–Western Pomerania (LALLF M-V) and gained governmental approval under the registration numbers LVL MV TSD/7221.3-1-029/22 and 7221.3-1-003/22. All mouse experiments were performed in accordance with the guidelines of the German animal protection law and were approved by the state of Baden-Württemberg (Regierungspräsidium Freiburg; reference number: 35-9185.81/G-19/05).

Animals

One-day-old chickens, 1-day-old turkeys, ferrets as well as C57BL/6 (B6) mice and human MxA transgenic (hMxA^{tg/tg}) mice were used for this study. Chicks were bred at the FLI from SPF-chicken eggs (VALO-BioMedia, Germany) and 1-day-old turkeys were ordered and shipped on hatching day from a local breeding facility (Bösel) to the FLI. The ferrets were obtained from the in-house breeding program at the FLI. B6 mice were obtained from Janvier and hMxA^{tg/tg} mice were bred in-house at the Institute of Virology, Freiburg. All mice were housed in individually ventilated cages (Green Line, Tecniplast) with stable bedding (ZHK: TAPVEI® BEDDING), at a temperature of 20.2 ± 1.1 °C, a humidity of $55\% \pm 7.1\%$ and a 12 h:12 h light:dark cycle. The mice were fed ad libitum with food made from natural ingredients (Germany, altromin 1314). All animal work was performed in BSL3 containment facilities.

One-day-old chicken and turkey studies

At the day of hatching, 1-day-old turkeys were inoculated with 10^5 TCID₅₀ per animal and 1-day-old chicks were inoculated with $10^{3.9}$ TCID₅₀ per animal, calculated by back-titration of the original inoculum. All hatchlings were sampled daily via cloacal and oro-pharyngeal

swabs until 21 dpi or until the animal samples tested negative in a bat H9N2-specific RT-qPCR. Oro-pharyngeal and cloacal swabs were taken using plain swab sterile paper applicator cotton tips 164 C (Copan, Brescia, Italy). The swabs were immediately transferred into 1 mL of cell culture medium containing 1% Baytril (Bayer, Leverkusen, Germany), 0.5% lincomycin (WDT, Garbsen, Germany) and 0.2% amphotericin/gentamycin (Fisher Scientific Waltham, MA, USA). After euthanasia, nasal conchae and colon organ samples were taken for investigation of viral genome loads via RT-qPCR analysis in the respective organs. Clinical status of the animals was checked daily.

Ferret study

18 adult ferrets (*Mustela putorius furo*, 10 females and 8 males, aged > 0.5 years) were housed in multi-connected cage units. Before inoculation, blood samples and nasal washings were collected to confirm naivety to IAV of all animals via serological analysis (ELISA) and RT-qPCR. Only one ferret showed some weak reactivity in the pre-experimental NP-ELISA, but was included in the study because of its low seropositivity, which could be due to a previously unrecognized IAV infection or an unspecific ELISA reactivity. However, there was no indication of any H9N2 serology before inoculation. Body weight, body temperature as well as physical condition of all animals was monitored regularly throughout the animal trial. Nasal washing samples were taken under a short-term isoflurane inhalation anesthesia by applying 750 μL of PBS into each nostril and collecting the efflux. Rectal swabs were taken using plain swab sterile paper applicator cotton tips 164 C (Copan). The swabs were immediately transferred into 1 mL of cell culture medium containing 1% Baytril (Bayer, Leverkusen, Germany), 0.5% lincomycin (WDT, Garbsen, Germany) and 0.2% amphotericin/gentamycin (Fisher Scientific Waltham, MA, USA). After 1 week of acclimatization to their new environment (0 dpi), 15 ferrets were intranasally inoculated with $10^{4.8}$ TCID₅₀ per animal in a 200 μL volume (calculated by back-titration of the original material). The inoculum was evenly distributed into each nostril (~ 100 μL per nostril). At 1 dpi, three naïve contact animals were co-housed in the multi-connected cage units of the donor ferrets to determine direct virus transmission. All animals were sampled via nasal washings and rectal swabs daily until 10 dpi and afterwards every second day until 21 dpi or until the samples tested negative via bat H9N2 specific RT-qPCR analysis. Clinical signs of disease (nasal discharge, reduced activity, fever, neurological symptoms and dyspnea), rectal body temperature and body weight were monitored daily. At 6 dpi, in the acute phase of the infection, six donor ferrets were euthanized and subject to necropsy for pathomorphological investigation and analysis of viral genome loads in the upper and lower respiratory organs, as well as in the intestinal tract. The residual animals were kept until the end of the study at 21 dpi to allow for seroconversion. Nasal conchae organ samples from animals euthanized at 21 dpi were analyzed with a bat H9N2-specific RT-qPCR.

Mouse study

For infection experiments, 15 B6 mice (7 females and 8 males, aged 6–10 weeks) and 14 hMxA^{tg/tg} mice (7 females and 7 males, aged 6–10 weeks) were anaesthetized with a mixture of ketamine (100 mg per g body weight) and xylazine (5 mg per g body weight) administered intraperitoneally and were subsequently inoculated intranasally with 40 μL of the indicated virus dose diluted in Opti-MEM containing 0.3% BSA. For interferon pretreatment 2 μg per 100 μL IFN- α was administered subcutaneously 18 h prior to challenge with the indicated virus. Throughout the experiment, mice were monitored daily for changes in body weight and other signs of disease. At 3 dpi mice were sacrificed and the lung was dissected. Organs were homogenized in 1 mL PBS by three subsequent rounds of mechanical treatment for 25 s each at 6.5 ms^{-1} . Tissue debris was removed by centrifuging homogenates for

5 min at $2.400 \times g$ at 4°C and samples were stored at -80°C until further processing. Viral organ titers were determined by plaque assay.

Propagation of bat H9N2 virus isolates from turkey samples

For isolation of bat H9N2 from turkey hatchlings, swab material was used for inoculation of embryonated chicken eggs. Briefly, $200\ \mu\text{l}$ of selected animal samples were transferred into the allantoic cavity of embryonated SPF-chicken eggs (three eggs per sample), followed by incubation for 5 days at 37°C . Viral genome material was extracted from the allantoic fluid and detected by RT-qPCR analysis.

Pathomorphology and immunohistochemistry

For the ferret histopathology, nasal conchae, trachea, right cranial, medial and caudal lung lobes as well as the colon were sampled. Tissues were fixed in 10% neutral buffered formalin, embedded in paraffin wax and cut at $3\ \mu\text{m}$ sections. To assess tissue architecture and cell morphology sections were stained with hematoxylin and eosin following standard procedures. For viral antigen detection immunohistochemistry was performed using an in house derived rabbit polyclonal primary antibody directed against the influenza nucleoprotein (NP, 1:750)³⁷. Lesions and cellular viral antigen localization were determined and evaluated by a board-certified pathologist (DiplACVP).

To analyze the cellular tropism of IAV infection in human lung tissue samples, tissues were fixed with 4% paraformaldehyde for 48 h, embedded in paraffin and processed for immunohistochemistry. Lung tissue was then blocked with 5% adequate serum and incubated with primary antibodies directed to CD68 (abcam, Cambridge, UK, 1:50), HT2-280 (terrace biotech, 1:200) and EMP2 (atlas antibodies, 1:50). Viral antigens were stained with polyclonal antibodies to IAV (Serotec, Puchheim, Germany, 1:50) conjugated to a fluorophore (DyLight 488, Thermo Fisher). Primary antibodies were detected using a corresponding secondary labeling kits (OPAL Polaris, Akoyabio) and nuclear counterstaining was performed using DAPI (Sigma, Hamburg, Germany). Finally tissue sections were mounted in Mowiol, and analyzed using a LSM 780 spectral confocal microscope (objectives 63x Plan-Apochromat/oil, NA 1.4, Zeiss, Germany).

Experimental sample work-up and analysis

Animal organ samples of about $0.1\ \text{cm}^3$ size were first homogenized in a 2 mL Eppendorf-tube containing 1 mL of Hank's balanced salts MEM and Earle's balanced salts MEM (2 mM L-glutamine, $850\ \text{mg}\ \text{L}^{-1}$ NaHCO_3 , $120\ \text{mg}\ \text{L}^{-1}$ sodium pyruvate, and 1% penicillin-streptomycin) at 300 Hz using a Tissuelyser II (Qiagen, Hilden, Germany). From each homogenized organ, swab or nasal wash sample, $100\ \mu\text{l}$ was extracted via the NucleoMag Vet kit (Macherey&Nagel, Düren, Germany) according to the manufacturer's instructions on a Biosprint 96 platform (Qiagen). Viral RNA was detected by RT-qPCR using bat H9N2-specific primers and probes³⁸. Absolute quantification was done using a standard of known concentrations, corresponding to the RNA of the original virus used for inoculation. Quantification was established by the QX200 Droplet Digital PCR System in combination with the 1-Step RT-ddPCR Advanced Kit for Probes (BioRad, Hercules, CA, US). Viral titers of ferret nasal washing samples were determined by TCID₅₀ endpoint dilution assay on MDCKII cells.

Human sera collected before and after seasonal influenza vaccination

The observational study protocol IRB-16-00772 was reviewed and approved by the Mount Sinai Hospital Institutional Review Board. All study participants provided written informed consent before biospecimens, and data were collected. Permissions to store and share biospecimen were also obtained from all participants. All specimens were coded before processing and analysis. Whole blood was collected through venipuncture into serum separator tubes and sera were stored at -80°C until analysis.

Serology

Serological analysis of blood samples from all animals at respective blood collection time points was performed by using a commercial IAV-specific enzyme-linked immunosorbent assay (ELISA) detecting NP-specific antibodies (ID-Vet, Montpellier, France) according to the manufacturer's instructions. The antibody titers were expressed as "% inhibition", which was calculated as $((\text{OD}_{450}\ \text{negative control} - \text{OD}_{450}\ \text{sample}) / \text{OD}_{450}\ \text{negative control}) \times 100$.

Neutralizing antibody titers were determined in a virus neutralization test (VNT). Briefly, MDCK cells seeded and grown in 96-well plates 24 h before infection. Serum samples were serially diluted in DMEM containing $1\ \mu\text{g}\ \text{mL}^{-1}$ TPCK-treated trypsin and then mixed with $100\ \text{TCID}_{50}\ \text{mL}^{-1}$ of either bat or chicken H9N2. After incubation for 2 h at 37°C and 5% CO_2 , the serum-virus mixture was transferred onto MDCK cells and incubated for 72 h. Neutralization was evaluated by light microscopy for the absence of specific cytopathic effect (CPE), and the corresponding VNT titer was determined from the last serum dilution in which no CPE was observed.

ELISAs with human sera against a recombinant version of the N2 NA of H9N2 virus A/bat/Egypt/381OP/2017 were performed as described in detail before³⁹. Recombinant NA from human seasonal H3N2 strain A/Kansas/14/2017 was used to show positive reactivity, recombinant NA from the Wuhan spiny eel influenza virus⁴⁰ (to which humans are naïve) was used as contrast to show negative reactivity. Recombinant proteins were expressed as described previously⁴¹. Sera collected from 15 study participants before and after receiving the 2022/23 seasonal influenza vaccination were used to determine reactivity to N2 from H9N2, N2 from seasonal H3N2 or to the Wuhan spiny eel influenza virus NA. Monoclonal antibody IG01⁴² was used as positive control in all cases.

Reporting summary

Further information on research design is available in the Nature Portfolio Reporting Summary linked to this article.

Data availability

The data generated in this study are provided in the Supplementary Information/Source Data file. PDB code: [2Q06](#) and GenBank accession numbers: [MH376902](#) to [MH376909](#) were used in this study. Source data are provided with this paper.

References

- Long, J. S., Mistry, B., Haslam, S. M. & Barclay, W. S. Host and viral determinants of influenza A virus species specificity. *Nat. Rev. Microbiol.* **17**, 67–81 (2019).
- Letko, M., Seifert, S. N., Olival, K. J., Plowright, R. K. & Munster, V. J. Bat-borne virus diversity, spillover and emergence. *Nat. Rev. Microbiol.* **18**, 461–471 (2020).
- Tong, S. et al. A distinct lineage of influenza A virus from bats. *Proc. Natl Acad. Sci. USA* **109**, 4269–4274 (2012).
- Tong, S. et al. New world bats harbor diverse influenza A viruses. *PLoS Pathog* **9**, e1003657 (2013).
- Kandeil, A. et al. Isolation and characterization of a distinct influenza A virus from Egyptian bats. *J. Virol.* **93**, e01059–18 (2019).
- Ciminski, K., Pfaff, F., Beer, M. & Schwemmler, M. Bats reveal the true power of influenza A virus adaptability. *PLoS Pathog* **16**, e1008384 (2020).
- Homme, P. J. & Easterday, B. C. Avian influenza virus infections. I characteristics of influenza A-Turkey-Wisconsin-1966 virus. *Avian Dis.* **14**, 66–74 (1970).
- Afifi, M. A., El-Kady, M. F., Zoelfakar, S. A. & Abdel-Moneim, A. S. Serological surveillance reveals widespread influenza A H7 and H9 subtypes among chicken flocks in Egypt. *Trop. Anim. Health Prod.* **45**, 687–690 (2013).

9. Li, C. et al. Genetic evolution of influenza H9N2 viruses isolated from various hosts in China from 1994 to 2013. *Emerg. Microbes Infect.* **6**, e106 (2017).
10. Dong, G. et al. Phylogenetic diversity and genotypical complexity of H9N2 influenza A viruses revealed by genomic sequence analysis. *PLoS One* **6**, e17212 (2011).
11. Cong, Y. L. et al. Swine infection with H9N2 influenza viruses in China in 2004. *Virus Genes* **36**, 461–469 (2008).
12. Zhang, C. et al. Avian influenza virus H9N2 infections in farmed minks. *Virology* **12**, 180 (2015).
13. WHO. *Avian Influenza Weekly Update Number 877, Page 1*. https://www.who.int/docs/default-source/wpro---documents/emergency/surveillance/avian-influenza/ai_20230106.pdf?sfvrsn=5f006f99_108 (2023).
14. Freidl, G. S. et al. Serological evidence of influenza A viruses in frugivorous bats from Africa. *PLoS One* **10**, e0127035 (2015).
15. Rademan, R., Geldenhuys, M. & Markotter, W. Detection and characterization of an H9N2 influenza A virus in the Egyptian rousette bat in Limpopo, South Africa. *Viruses* **15**, 498 (2023).
16. Gao, R. et al. The comparison of pathology in ferrets infected by H9N2 avian influenza viruses with different genomic features. *Virology* **488**, 149–155 (2016).
17. Wan, H. et al. Replication and transmission of H9N2 influenza viruses in ferrets: evaluation of pandemic potential. *PLoS One* **3**, e2923 (2008).
18. Zitzow, L. A. et al. Pathogenesis of avian influenza A (H5N1) viruses in ferrets. *J. Virol.* **76**, 4420–4429 (2002).
19. Zhu, H. et al. Infectivity, transmission, and pathology of human-isolated H7N9 influenza virus in ferrets and pigs. *Science* **341**, 183–186 (2013).
20. Taubenberger, J. K. & Morens, D. M. The pathology of influenza virus infections. *Annu. Rev. Pathol.* **3**, 499–522 (2008).
21. Weinheimer, V. K. et al. Influenza A viruses target type II pneumocytes in the human lung. *J. Infect. Dis.* **206**, 1685–1694 (2012).
22. Zimmermann, P., Manz, B., Haller, O., Schwemmler, M. & Kochs, G. The viral nucleoprotein determines Mx sensitivity of influenza A viruses. *J. Virol.* **85**, 8133–8140 (2011).
23. Manz, B. et al. Pandemic influenza A viruses escape from restriction by human MxA through adaptive mutations in the nucleoprotein. *PLoS Pathog* **9**, e1003279 (2013).
24. Ashenberg, O., Padmakumar, J., Doud, M. B. & Bloom, J. D. Deep mutational scanning identifies sites in influenza nucleoprotein that affect viral inhibition by MxA. *PLoS Pathog* **13**, e1006288 (2017).
25. Deeg, C. M. et al. In vivo evasion of MxA by avian influenza viruses requires human signature in the viral nucleoprotein. *J. Exp. Med.* **214**, 1239–1248 (2017).
26. Nachbagauer, R. et al. Defining the antibody cross-reactome directed against the influenza virus surface glycoproteins. *Nat. Immunol.* **18**, 464–473 (2017).
27. Meade, P. et al. Influenza virus infection induces a narrow antibody response in children but a broad recall response in adults. *mBio* **11**, e03243–19 (2020).
28. Group, S. H. W. Assessing the fitness of distinct clades of influenza A (H9N2) viruses. *Emerg. Microbes Infect.* **2**, e75 (2013).
29. Li, X. et al. Genetics, receptor binding property, and transmissibility in mammals of naturally isolated H9N2 Avian Influenza viruses. *PLoS Pathog* **10**, e1004508 (2014).
30. Belser, J. A. et al. Genetically and antigenically divergent influenza A(H9N2) viruses exhibit differential replication and transmission phenotypes in mammalian models. *J. Virol.* **94**, e00451–20 (2020).
31. Zhang, X. et al. H9N2 influenza virus spillover into wild birds from poultry in China bind to human-type receptors and transmit in mammals via respiratory droplets. *Transbound. Emerg. Dis.* **69**, 669–684 (2022).
32. Kirkeby, S., Martel, C. J. & Aasted, B. Infection with human H1N1 influenza virus affects the expression of sialic acids of metaplastic mucous cells in the ferret airways. *Virus Res.* **144**, 225–232 (2009).
33. de Graaf, M. & Fouchier, R. A. Role of receptor binding specificity in influenza A virus transmission and pathogenesis. *EMBO J.* **33**, 823–841 (2014).
34. Ciminski, K., Chase, G. P., Beer, M. & Schwemmler, M. Influenza A viruses: understanding human host determinants. *Trends Mol. Med.* **27**, 104–112 (2021).
35. Parvin, R. et al. Co-subsistence of avian influenza virus subtypes of low and high pathogenicity in Bangladesh: challenges for diagnosis, risk assessment and control. *Sci. Rep.* **9**, 8306 (2019).
36. Hoffmann, E., Krauss, S., Perez, D., Webby, R. & Webster, R. G. Eight-plasmid system for rapid generation of influenza virus vaccines. *Vaccine* **20**, 3165–3170 (2002).
37. Abdelwhab, el-S. M. et al. Prevalence of the C-terminal truncations of NS1 in avian influenza A viruses and effect on virulence and replication of a highly pathogenic H7N1 virus in chickens. *Virulence* **7**, 546–557 (2016).
38. Halwe, N. J. et al. Egyptian fruit bats (*Rousettus aegyptiacus*) were resistant to experimental inoculation with avian-origin influenza A virus of subtype H9N2, but are susceptible to experimental infection with bat-borne H9N2 virus. *Viruses* **13**, 672 (2021).
39. Carreno, J. M. et al. Activity of convalescent and vaccine serum against SARS-CoV-2 Omicron. *Nature* **602**, 682–688 (2022).
40. Arunkumar, G. A. et al. Functionality of the putative surface glycoproteins of the Wuhan spiny eel influenza virus. *Nat. Commun.* **12**, 6161 (2021).
41. Margine, I., Palese, P. & Krammer, F. Expression of functional recombinant hemagglutinin and neuraminidase proteins from the novel H7N9 influenza virus using the baculovirus expression system. *J. Vis. Exp.* **81**, 2–8.e51112 (2013).
42. Stadlbauer, D. et al. Broadly protective human antibodies that target the active site of influenza virus neuraminidase. *Science* **366**, 499–504 (2019).

Acknowledgements

We thank M. Grawe, P. Zitzow, S. Schuparis, R. Brandt, G. Heins and K. Hellwig for outstanding technical assistance, F. Klipp, S. Kiepert, D. Fiedler and C. Lipinski for their dedicated animal care, and G. Chase for excellent assistance with manuscript preparation, and A. Breithaupt for excellent assistance in pathology-related questions concerning the interpretation of our data. The work was funded by grants from the European Research Council (ERC) to M.S. (NUMBER 882631—Bat Flu), the Deutsche Forschungsgemeinschaft (DFG) with grants to M.S. (SCHW 632/17-2), M.B. (BE 5187/4-2), T.W., S.H. and A.C.H. (SFB-TR 84), the Federal Ministry of Education and Research (BMBF) with grants to S.H., A.C.H. and T.W. (RAPID), the Einstein Foundation EC3R and Charité^{3R} with grants to S.H. and A.C.H. and by the Medical Faculty, University of Freiburg through the “Hans A. Krebs Medical Scientist Programme” to K.C. Protein production and assays with human sera and recombinant proteins was supported by the National Institute of Allergy and Infectious Disease (NIAID) Centers of Excellence for Influenza Research and Response (CEIRR) contract 75N93021C00014.

Author contributions

N.J.H., D.H. and M.Be. conceived the study. N.J.H., J.S., L.U. and D.H. designed and performed turkey, chicken and ferret experiments. J.S.E. and L.U. performed ferret pathology. C.M., M.T., M.Bu., S.H., A.H. and T.W. designed and performed human lung explant infection experiments. L.H., J.F. and K.C. designed and performed mouse infections. P.B., M.L., A.A., J.M.C., V.S. and F.K. collected serum samples, and designed and performed serological analysis. A.K., R.E.S., M.A.A. and

G.K. provided reagents. S.C. performed sequence analysis. N.J.H., M.S., K.C. and M.Be. wrote the original draft. N.J.H., J.S.E., L.U., F.K., M.S., K.C., D.H. and M.Be. reviewed and edited the paper. T.W., S.H., A.C.H., M.S., K.C. and M.Be. acquired funds.

Funding

Open Access funding enabled and organized by Projekt DEAL.

Competing interests

The Icahn School of Medicine at Mount Sinai has filed patent applications relating to influenza virus vaccines, SARS-CoV-2 serological assays and SARS-CoV-2 vaccines which list Florian Krammer as co-inventor. Viviana Simon is also listed as co-inventor on patent applications for SARS-CoV-2 serological assays. Mount Sinai has spun out companies, Kantaro and Castlevax, to market the SARS-CoV-2 related technologies. Florian Krammer has consulted for Merck and Pfizer (before 2020), and is currently consulting for Pfizer, Seqirus, 3rd Rock Ventures, GSK and Avimex. The Krammer laboratory is also collaborating with Pfizer on animal models of SARS-CoV-2 and with Dynavax on universal influenza virus vaccines. All other authors declare no competing interests.

Additional information

Supplementary information The online version contains supplementary material available at <https://doi.org/10.1038/s41467-024-47455-6>.

Correspondence and requests for materials should be addressed to Kevin Ciminski, Donata Hoffmann or Martin Beer.

Peer review information *Nature Communications* thanks the anonymous reviewers for their contribution to the peer review of this work. A peer review file is available.

Reprints and permissions information is available at <http://www.nature.com/reprints>

Publisher's note Springer Nature remains neutral with regard to jurisdictional claims in published maps and institutional affiliations.

Open Access This article is licensed under a Creative Commons Attribution 4.0 International License, which permits use, sharing, adaptation, distribution and reproduction in any medium or format, as long as you give appropriate credit to the original author(s) and the source, provide a link to the Creative Commons licence, and indicate if changes were made. The images or other third party material in this article are included in the article's Creative Commons licence, unless indicated otherwise in a credit line to the material. If material is not included in the article's Creative Commons licence and your intended use is not permitted by statutory regulation or exceeds the permitted use, you will need to obtain permission directly from the copyright holder. To view a copy of this licence, visit <http://creativecommons.org/licenses/by/4.0/>.

© The Author(s) 2024

¹Institute of Diagnostic Virology, Friedrich-Loeffler-Institut, 17493 Greifswald, Insel Riems, Germany. ²Institute of Virology, Medical Center-University of Freiburg, 79104 Freiburg, Germany. ³Faculty of Medicine, University of Freiburg, 79104 Freiburg, Germany. ⁴Department of Experimental Animal Facilities and Biorisk Management, Friedrich-Loeffler-Institut, 17493 Greifswald, Insel Riems, Germany. ⁵Unit 17, Influenza and Other Respiratory Viruses, Robert Koch-Institut, Seestraße 10, 13353 Berlin, Germany. ⁶HELIOS Clinic Emil von Behring, Department of Pneumology and Department of Thoracic Surgery, Chest Hospital Heckeshorn, Berlin, Germany. ⁷Department of Microbiology, Icahn School of Medicine at Mount Sinai, New York, NY 10029, USA. ⁸Center for Vaccine Research and Pandemic Preparedness (C-VaRPP), Icahn School of Medicine at Mount Sinai, New York, NY, USA. ⁹Department of Pathology, Molecular and Cell Based Medicine, Icahn School of Medicine at Mount Sinai, New York, NY, USA. ¹⁰Division of Infectious Diseases, Department of Medicine, Icahn School of Medicine at Mount Sinai, New York, NY, USA. ¹¹The Global Health and Emerging Pathogens Institute, Icahn School of Medicine at Mount Sinai, New York, NY, USA. ¹²Center of Scientific Excellence for Influenza Virus, Institute of Environmental Research and Climate Changes, National Research Centre, Giza, Egypt. ¹³Human Link DMCC, Dubai, United Arab Emirates. ¹⁴Department of Infectious Diseases and Respiratory Medicine, Charité—Universitätsmedizin Berlin, corporate member of Freie Universität Berlin and Humboldt Universität zu Berlin, Berlin, Germany. ✉ e-mail: kevin.ciminski@uniklinik-freiburg.de; donata.hoffmann@fli.de; martin.beer@fli.de